Loading rate effects on mode-I delamination in glass/epoxy and glass/CNF/epoxy laminated composites

Ekhtiyari, Amin; Shokrieh, Mahmood M.; Alderliesten, René

DOI
10.1016/j.engfracmech.2020.106908

Publication date
2020

Document Version
Final published version

Published in
Engineering Fracture Mechanics

Engineering Fracture Mechanics 228 (2020) 106908

Contents lists available at ScienceDirect

Engineering Fracture Mechanics

journal homepage: www.elsevier.com/locate/engfracmech

Loading rate effects on mode-I delamination in glass/epoxy and glass/CNF/epoxy laminated composites

Amin Ekhtiyari[a], Mahmood M. Shokrieh[a,*], René Alderliesten[b]

[a] Composites Research Laboratory, Center of Excellence in Experimental Solid Mechanics and Dynamics, School of Mechanical Engineering, Iran University of Science and Technology, Tehran 16846-13114, Iran

[b] Structural Integrity & Composites Group, Faculty of Aerospace Engineering, Delft University of Technology, Kluyverweg 1, Delft, HS 2629, The Netherlands

ARTICLE INFO

Keywords:
Mode-I delamination
Fracture toughness
Rate effect
Fiber bridging
Hybrid reinforcement
Carbon nanofibers

ABSTRACT

The main objective of the present study is to assess the loading rate effects on mode-I delamination growth in glass/epoxy laminated composites. Furthermore, hybrid reinforcement of these composites by incorporating carbon nanofibers (CNFs) was followed to enhance the interlaminar fracture resistance and affect its loading rate sensitivity. Experiments on DCB specimens made of glass/epoxy and glass/CNF/epoxy laminated composites were conducted by varying the loading rate from standard quasi-static testing up to 200 mm/sec crosshead speed in a servo-hydraulic test machine. More than 21% decrease was observed in the propagation fracture toughness of the glass/epoxy samples due to loading rate elevation in the studied range. Moreover, the results of the present study clearly show the benefits of CNF modification, not only in enhancing the fracture toughness but also in reducing the loading rate dependency. Adding CNFs to glass/epoxy composites caused 32.8% and 13.5% increase in the quasi-static values of the initiation- and propagation-interlaminar fracture toughness (G_{IC}), respectively. Also, owing to CNF incorporation, the maximum drop in the propagation fracture toughness at elevated loading rates was decreased to 8%. Fractography inspections were performed to provide an in-depth explanation for the observed loading rate effects and the advantages of CNF reinforcement.

1. Introduction

The loading rate dependency of delamination growth has been investigated in several research works reviewed by May [1]. Experiments on double cantilever beam (DCB) specimens were standardized for mode-I interlaminar fracture toughness (G_{IC}) characterization of fiber-reinforced plastics under quasi-static loads [2]. Although no standard test procedure is introduced for dynamic loadings up to now, the DCB configuration has been the most common test set-up for the rate dependency examination of G_{IC} at intermediate rates of loading [3–9]. This configuration has even been modified for further studies at higher loading rates [10,11]. Notwithstanding the number of previous researches on the rate dependency analysis of delamination in carbon fiber reinforced plastics (CFRPs), the available experimental data are rather controversial and there is no general agreement on the loading rate effects. Whereas a number of researchers reported an increase in G_{IC} with loading rate [3,6,12], some others found reduced fracture resistance at increased loading rates [4,7,9,11]. In contrast, no significant loading-rate dependency of fracture toughness was observed in a few different research works [13,14].

* Corresponding author.
E-mail address: shokrieh@iust.ac.ir (M.M. Shokrieh).

https://doi.org/10.1016/j.engfracmech.2020.106908
Received 20 September 2019; Received in revised form 23 January 2020; Accepted 24 January 2020
Available online 25 January 2020

On the other hand, only limited information is available in the literature about the loading rate effects on mode-I delamination in glass/epoxy composites. For instance, Benmedakhene et al. [15] conducted simple-cantilever beam (SCB) tests in a drop tower. Compared to the results of low rate DCB tests, they observed an increase in the initiation and propagation values of G_{IC}. This behavior was attributed to a failure propagation scheme change from primary crack growth in the epoxy matrix at low-velocity DCB tests to crack propagation in the fiber/matrix and inter-ply interfaces at high-velocity SCB tests. Conversely, a transition from fiber/matrix interface failure to resin rich brittle fracture was described as the reason for a reduced G_{IC} at higher loading rates in carbon/epoxy samples [9]. The interlaminar fracture behavior of glass/epoxy laminates at quasi-static loading was recurrently focused in preceding published papers [16,17]. It was shown that fiber bridging is a dominant energy dissipating mechanism in these composites [17]. On the other hand, in some rate dependency studies of delamination in CFRPs [9,18,19], it was claimed that fiber bridging can obscure the rate dependency of fracture toughness. Nonetheless, the reduced delamination resistance at elevated rates found in [11] was ascribed to a lower extent of fiber bridging. No explanation of the contribution of fiber bridging and its interaction with the loading rate in the delamination of glass/epoxy composite was delivered in reference [15]. On account of these contradictory results in the literature, a further experimental investigation is needed to achieve a better understanding of the rate dependency of delamination growth behavior in glass/epoxy composites.

Additionally, another research gap that needs to be more explored is the rate dependency study of delamination in hybrid reinforced composites. In order to address the delamination susceptibility of fiber-reinforced plastics (FRPs), different methods have been studied, including matrix modification by nano-reinforcements [20–24]. It has been frequently reported that the quasi-static G_{IC} of fiber-reinforced epoxies can be increased by adding nanofillers without compromising their outstanding in-plane mechanical characteristics. Due to their high aspect ratio and superior mechanical properties, Carbon nanofibers (CNFs), as a promising candidate material have been utilized in numerous studies [22–28]. This extensive research background reveals a good potential for adding CNFs to the pure resin in laminated FRPs as a beneficial and low-cost reinforcing method to improve G_{IC}. However, to the best knowledge of the authors, the capability of nano-reinforcements to enhance the interlaminar fracture resistance of laminated composites undergoing moderate to high loading rates have yet to be studied. Therefore, a subsequent part of this research focused on using CNFs for improving the mode-I fracture toughness of laminated glass/epoxy composites and assessment of their performance at increased loading rates.

To sum up, the purpose of this study was two-fold: (a) to conduct a thorough investigation into loading rate effects on mode-I delamination growth in glass/epoxy laminated composites in presence of large-scale fiber bridging and quantitative measurement of the extent of process zone at elevated rates and (b) to examine the effect of adding CNFs to the epoxy resin as a promising method to enhance the delamination resistance of FRPs at loading rates ranging from quasi-static tests up to 200 mm/sec. The experimental results showed that while the glass/epoxy composite suffers from a fracture resistance drop at elevated loading rates, the studied CNF-modification technique succeeded to improve the G_{IC} as well as decrease its rate sensitivity.

2. Experimental procedure

2.1. Materials and fabrication process

Unidirectional E-glass fibers and Razeen® LR 1100 epoxy resin (a bisphenol A/epichlorohydrin derived liquid epoxy resin) hardened with Epikure 3234 (Teta) curing agent by 100:13 wt ratio were used to manufacture 24-ply E-glass/epoxy fiber-reinforced laminates by the hand lay-up method. The density of E-glass fibers and epoxy resin are 2.56 g/cm^3 and 1.16 g/cm^3, respectively. During the lay-up process, a thin Teflon film of 20 μm thickness was placed at the mid-plane of the laminate to serve as the delamination starter crack. The laminates were cured at room temperature for 2 days followed by a post-cure scheme of 1 h at 80 °C and 2 h at 110 °C to ensure a complete curing process and achieve the best mechanical properties. The density of the resulted composite was 1.77 g/cm^3 according to ASTM D792-13. Fiber volume fraction measurement based on ASTM D3171 standard and burn off procedure resulted in an average value of 46.1% for four representative samples. According to the ASTM D2734 standard, the void content in the composite samples was less than 3% for all the samples. DCB specimens with the standard width of 25 mm and an initial crack length of 50 mm were cut from the composite plates using a diamond saw. The average thickness of the samples was 4.7 mm.

2.2. Preparation of glass/CNF/epoxy composite specimens

Carbon nanofibers with an average diameter of 20–80 nm and a minimum length of 30 μm giving an aspect ratio in the range of 350–1500, were provided by Grupo Antolin SL, Spain. These nanofillers were utilized for hybrid reinforcement of the composite DCB specimens along the delamination growth path. Among different factors that may affect the mechanical properties of nano-reinforced composites, the optimum weight fraction of nanofillers and their uniform dispersion to avoid agglomeration have always been of great importance. On account of their high aspect ratio, CNFs and CNTs tend to easily agglomerate into clusters which may impair their ability to improve mechanical properties of nanocomposites [28–30]. As demonstrated by Shokrieh et al. [31,32], 0.25 wt% incorporation of CNFs in the epoxy matrix leads to an optimum improvement in the mechanical properties of the nano-modified resin. At higher contents of CNF, the uniform dispersion of nanofillers becomes less attainable and therefore consequent agglomerates of CNFs can nullify their beneficial effects on mechanical properties of the nanocomposite. Accordingly, the same CNF content of 0.25 wt% was used for the similar material system of CNF and epoxy matrix in the present study.

The CNF placement approach used in the present study is based on the idea that instead of adding nanofillers to the whole resin,

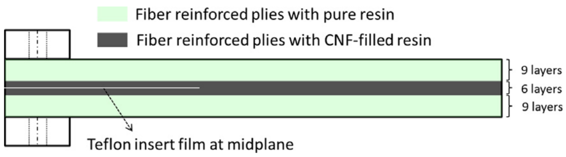

Fig. 1. Schematic representation of a DCB specimen with CNF-filled region around the mid-plane.

concentrating CNFs directly at the resin layer disposed around the fracture plane and along the delamination growth path can more efficiently affect the delamination growth with less consumption of the nanofillers. Inspired by the method of Zhu et al. [24], three adjacent layers above and below the mid-plane (Fig. 1) were impregnated with CNF-modified resin during the hand lay-up process.

A combination of high speed mechanical stirring and ultrasonic agitation was used to achieve a suitable dispersion of CNFs into epoxy. In this regard, the calculated weight of resin, required for the impregnation of the middle six layers of the composite laminate, was thoroughly mixed with 0.25 wt% CNF by mechanical stirring for 30 min at 2000 rpm. Then, the suspension was sonicated for 120 min in a Hielscher UP400S ultrasonic processor via a 14 mm diameter sonotrode. The output power and frequency of the sonicator were respectively set at 200 W and 12 kHz. During the sonication, the mixture container was held in an ice bath to prevent overheating of the suspension. The appropriate sonication time, which is a key parameter to achieve a good dispersion of CNFs with minimum damages imposed on them, depends on the filler content as well as the physical and chemical characteristics of the employed resin and nanofiller. An approach recommended by Chitsazzadeh et al. [33] and Shokrieh et al. [31], was used to find the optimized sonication time.

After sonication, the proper amount of hardener with a 13% mixing ratio by weight was added to the mixture and stirred gently for 15 min. This nano-filled resin was applied at the interlayer and the six layers symmetrically disposed around the mid-plane. The other 18 layers above and below the middle nano-reinforced region were impregnated with neat resin during the hand lay-up process. The same cure and post-cure processes of glass/epoxy composites were used for glass/CNF/epoxy composites. A schematic representation of DCB specimens with CNF-filled region around the mid-plane is shown in Fig. 1.

2.3. Test method, data acquisition, and data reduction

Using MTS 810 servo-hydraulic test machine, monotonic displacement controlled DCB tests were conducted at various crosshead speeds ranging from quasi-static to moderate rates of maximum 200 mm/sec. For quasi-static tests, the displacement rate was set at 1 mm/min as recommended by ASTM D 5528 standard [2]. In order to study the effect of loading rate in the scope of the present study, DCB tests were performed at three different applied velocities of 50 mm/s, 100 mm/s and 200 mm/s. DCB tests were repeated at least four times per loading rate for both glass/epoxy and glass/CNF/epoxy composite samples.

The test machine is equipped with a high-precision 1 kN HBM load cell which is sensitive enough to accurately measure dynamic loads. In addition, the load cell is connected to the stationary arm of the testing machine, as close to the specimen as possible. This measure has been suggested in some other high rate experimental studies to further reduce possible inherent dynamic effects [1]. The applied loads and displacements were recorded by a data acquisition unit. A 5 MP digital camera with an 80 mm lens and a maximum 200 Hz recording speed was used to monitor the crack evolution. In order to facilitate synchronization of the data, the load and displacement signals were sent from the test machine to the data logger accompanying the camera system. The camera was triggered manually before the test starts and the acquired signals of the load and displacement along with the synchronized image frame numbers were concurrently recorded by the camera system. The crack evolution was measured in the post-test analysis step using the open-source image processing program ImageJ. The DCB test configuration is shown in Fig. 2.

In ASTM D 5528, three methods are described to determine the onset of delamination growth initiation, i.e., NL point, VIS point, and 5% / MAX point. The NL point method normally represents a lower bound for G_{IC}, while in some physics-based studies it is

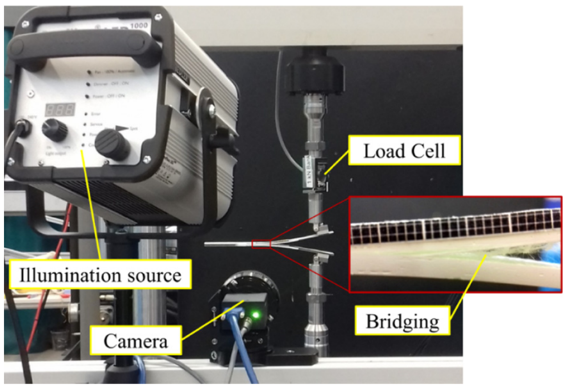

Fig. 2. The DCB test configuration.

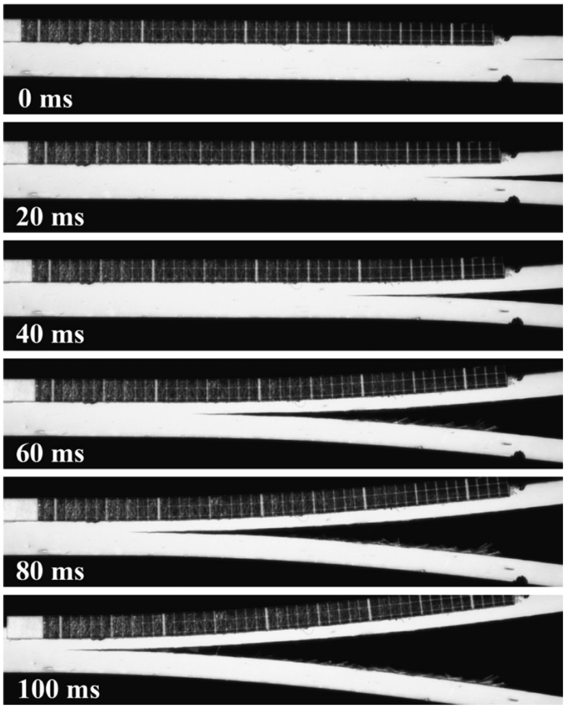

Fig. 3. The crack evolution response of a glass/epoxy DCB specimen tested at 200 mm/sec loading rate.

claimed that this value does not necessarily refer to the actual onset [34,35]. In the present study, the initiation value of G_{IC} at quasi-static and low-rate tests has been determined based on the NL point method. Classical data reduction methods are reported to be capable of providing reliable results for the analysis of DCB tests conducted at intermediate loading rates [1]. In the present study, the mode-I interlaminar strain energy release rate was calculated based on the modified beam theory as described in ASTM D5528. The calculations were done for any increment of at least 1 mm in delamination length to derive the R-curve.

It is worth mentioning that there may be concerns about the validity of G_{Ic} calculation while large scale fiber bridging occurs during delamination growth. In such a case, direct measurement of the path independent J-integral can be considered to account for the effect of the large fracture process zone. However, one should note that a limited difference between the values of G and J is expected based on the information available in the literature. Fracture energies obtained through LEFM or the J-integral method differed by no more than 5% in glass/epoxy composites in the case of large scale fiber bridging [36]. Moreover, assuming the value of J-integral very close to G_{Ic} did not impose a significant error on deriving a cohesive law and then in simulating delamination growth with finite element models in glass/epoxy composites similar to the one being studied here [37]. Thus, the G_{Ic} analysis as done here is sufficient to demonstrate the influence of the loading rate and CNF modification.

3. Results and discussion

3.1. Crack evolution and load–displacement response

The evolution of delamination at the time intervals of 20 ms for glass/epoxy DCB specimens tested at 200 mm/sec is illustrated in Fig. 3. The analysis of all the image sequences obtained at the highest loading rate confirmed that the symmetrical opening of the specimen arms had been fulfilled throughout the test. The 200 Hz capturing rate enabled the measurement of the crack length at every 5 ms. Although this frame rate may seem to be insufficient for accurate measurement of the instantaneous crack propagation velocity especially at the initiation, it was found adequate enough for deriving the R-curve, thanks to the main stable crack growth observed for both materials in the desired range of loading rates.

Typical load–displacement curves for glass/epoxy and glass/CNF/epoxy composite specimens, tested at minimum and maximum imposed loading rates, as well as delamination length versus displacement data points, are shown in Fig. 4. The data close to the average values among different repetitions in each case was selected to plot a clear figure. It should be mentioned that all experimental data of this study, including load–displacement response and synchronized crack evolution data were obtained through the image post-processing phase for all specimens at different rates and have been included in the online dataset accompanying this paper [38].

As shown in Fig. 4, there is an overall similarity between four load–displacement curves in which after initiation of delamination growth (deviation from linearity) load still increases up to a peak value and then starts a nearly stable descending trend. This behavior should be associated with the fiber bridging phenomenon. Regarding the effect of nano-reinforcement, the load values

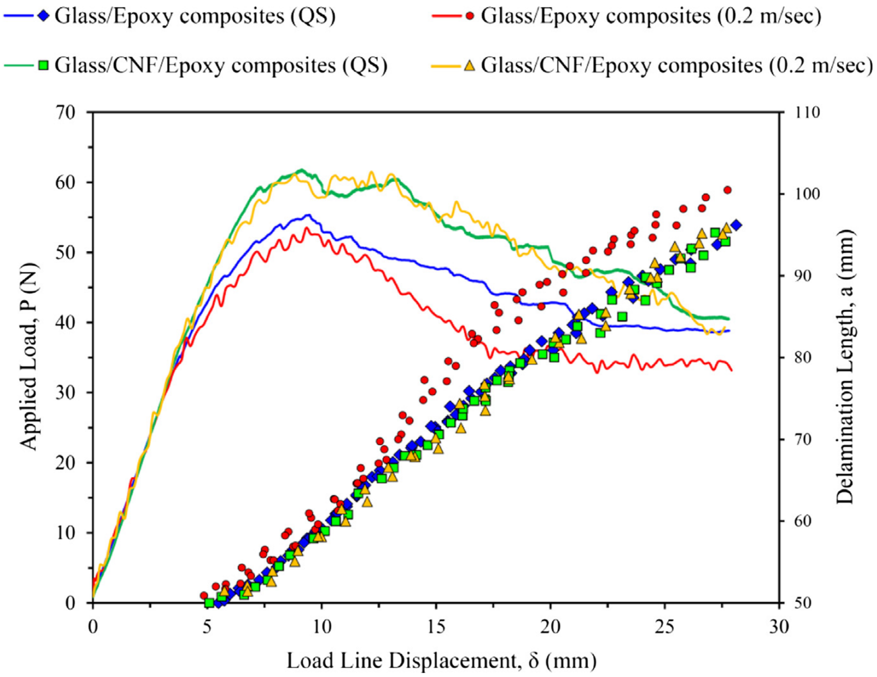

Fig. 4. The load and crack length evolution versus imposed far-field displacement for both glass/epoxy and glass/CNF/epoxy composite specimens tested at two different loading rates.

measured for the glass/CNF/epoxy composites (green curve) after initiation of delamination growth are remarkably higher than the values obtained for the glass/epoxy composites (blue curve) while they match in the linear part of the curves. The initial linear response is mainly affected by the longitudinal stiffness of specimen arms. Nano-additives are commonly expected to have a minor effect on the stiffness of FRPs in the fiber direction and therefore a similar linear elastic behavior resulted in both composites. From the crack evolution point of view, glass/CNF/epoxy composites data points (green squares) are placed beneath glass/epoxy composites data points (blue diamonds) in Fig. 4. The increased load along with the reduced delamination length for the same value of displacement indicates the enhanced fracture resistance due to nano-reinforcement which will be discussed later.

Fig. 4 reveals different rate dependency in the delamination growth behavior of the glass/epoxy and glass/CNF/epoxy composite specimens. In glass/epoxy composites, the softening part of the load–displacement curve accelerates at the elevated loading rate compared to the quasi-static case and the difference between two curves becomes more pronounced.

The discrepancy of the load–displacement curves for six different glass/epoxy specimens tested at maximum and minimum loading rates are shown in Fig. 5(a). Small dynamic oscillations at a 200 mm/sec loading rate cannot introduce a significant error to the analysis. It is apparent that an accelerated decrease in load magnitude after the peak happened for the three specimens at the elevated rate. This behavior is in accordance with the speeded increase in delamination length at this rate as illustrated in Fig. 4. In this figure, red circles represent the crack evolution data points for the tests with a 200 mm/sec loading rate on the three different specimens. Following an increment of about 15 mm in the delamination length, a fast-track growth profile starts in elevated rate tests. A transition from the development phase to saturation (steady-state propagation) phase in the fracture happens at approximately 65 mm of the delamination length which should be explained in conjunction with the fiber bridging. No clear rate dependency can be elucidated for the initiation stage due to advancing fiber bridges and possible crack insert effects. The propagation stage is where the hastened reductions in the load and jumps in the delamination length are observed at elevated-rate tests.

In contrast to the glass/epoxy composite specimens, there were no significant differences in the response of glass/CNF/epoxy composite samples at various loading rates. For this kind of composites, crack evolution results (see Fig. 4) and load–displacement curves (see Fig. 5(b)) at the minimum and maximum applied rates are within the scatter band of the experimental data.

3.2. R-curve analysis

The R-curve behavior of DCB specimens at quasi-static and maximum rate tests for glass/epoxy and glass/CNF/epoxy composite specimens are presented in Fig. 6. As a result of fiber bridging, the fracture toughness increases from the initial value up to a typical steady-state value ($G_{Ic}^{Prop.}$) and the curve becomes approximately plateau. In other words, the size of the zone behind the crack front, where fibers have bridged between adjacent crack faces, develops as the crack propagates. At the steady-state delamination growth, the bridging zone length reaches its maximum value. This bridging zone along with the zone of micro-cracks and plastic deformations in the vicinity of the crack tip, compose the total fracture process zone (l_{FPZ}^{ss}) which can be evaluated by the increment in delamination length till the fracture toughness reaches $G_{Ic}^{Prop.}$. The average values of propagation fracture toughness and the equivalent process zone

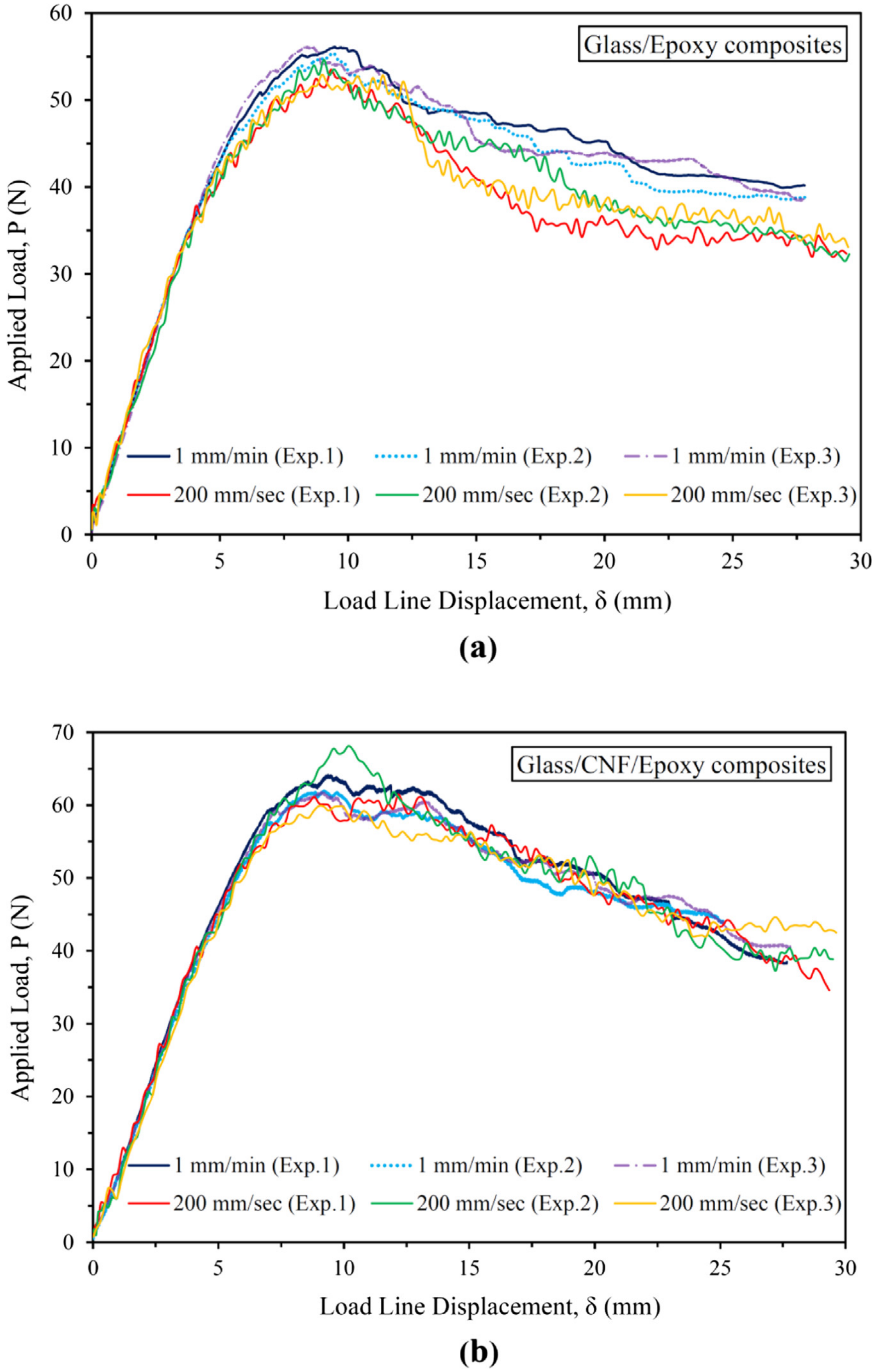

Fig. 5. Load-displacement curves for (a) glass/epoxy and (b) glass/CNF/epoxy composite specimens tested at quasi-static and 200 mm/sec loading rates.

length are denoted in Fig. 6.

It can be seen in Fig. 6-a that for glass/epoxy composites at 200 mm/sec rate, the R-curve tends to become plateau earlier at a significantly lower level of the fracture toughness and process zone length compared to their values at quasi-static tests. In quasi-static cases, the overall ascending trend of the strain energy release rate continues until higher values of the process zone length (around 22 mm). The fracture toughness in elevated rates starts fluctuation on the specified propagation value after developing a smaller process zone (around 13.5 mm). More drops from the average propagation fracture toughness are observed in high rate tests due to the longer crack jumps and related load falls. This observation which supports the rate dependency of fiber bridging, reported by Thorsson et al. [11], may dispute the generality of the claim that the presence of even small amounts of fiber bridging makes it

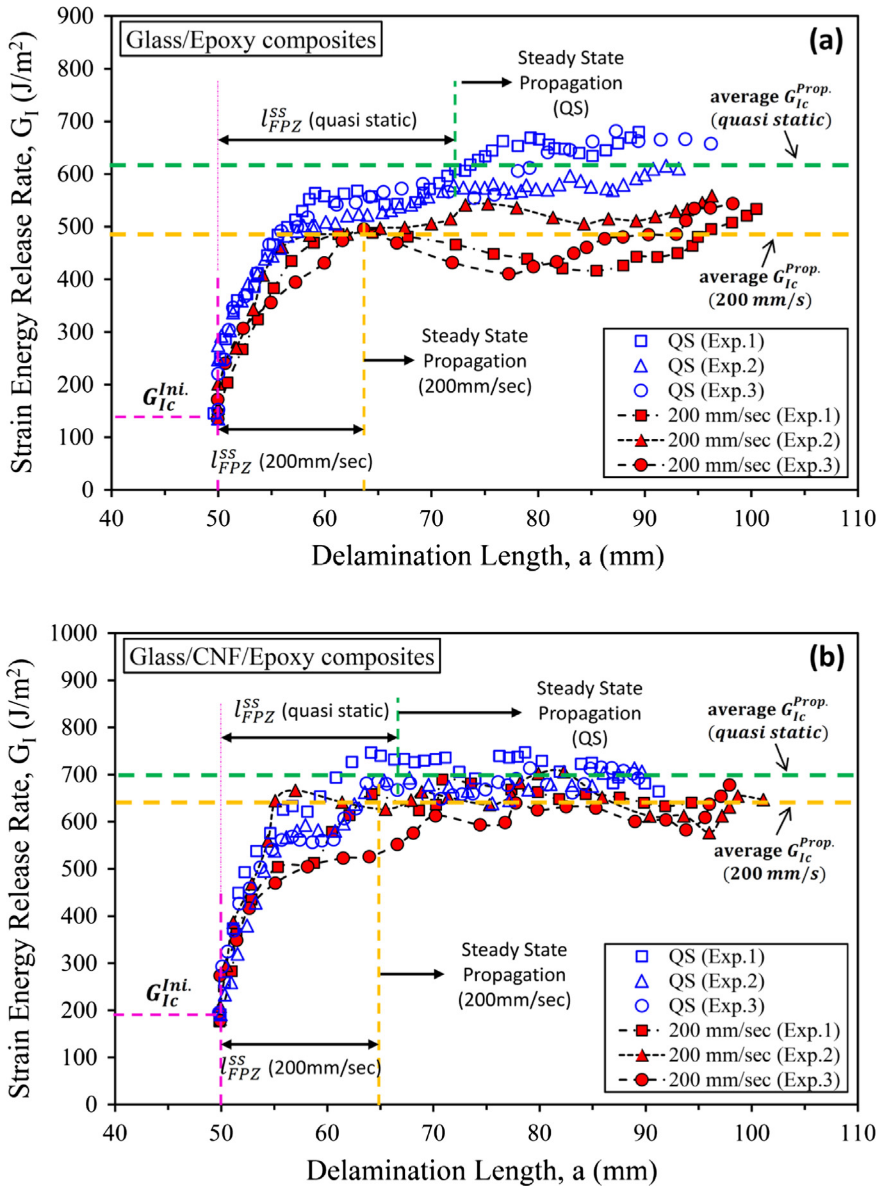

Fig. 6. The R-curve behavior of DCB specimens at quasi-static and 0.2 m/sec loading rates for (a) glass/epoxy and (b) glass/CNF/epoxy composite specimens.

difficult to observe any clear rate sensitivity in G_{IC} of unidirectional composites as asserted in the literature [9,18,19]. In other words, these results clearly show that although fiber bridging dominates the stable delamination growth process, its extent is evidently rate-dependent and decreases at high strain rates.

Comparing Fig. 6(a) and (b) demonstrates that the differences between the resistance behavior of glass/CNF/epoxy composite specimens at quasi-static and 200 mm/sec tests are notably less than that was observed for the glass/epoxy composite samples. This finding indicates that the toughening mechanisms contributed to form the steady-state process zone and increase the propagation fracture resistance in glass/CNF/epoxy composite specimens, were not considerably influenced by the loading rate within the chosen range.

The initiation and propagation values of strain energy release rates, as well as the steady-state process zone length of the two types of the specimen under various loading rates, are summarized in Table 1. At quasi-static loading, the results show that adding CNF increased $G_{Ic}^{Ini.}$ and $G_{Ic}^{Prop.}$ by 33.2% and 13.5% respectively. This enhancement is comparable to the achievements reported in [26]. Different mechanisms account for theses toughening effect will be discussed at the end of this section.

A clear comparison between average values of $G_{Ic}^{Prop.}$ for both materials at four different loading rates is illustrated in Fig. 7. At quasi-static loading, adding CNFS to composites increased $G_{Ic}^{Prop.}$ by more than 13.5% compared to the glass/epoxy composites. Although for both materials, $G_{IC}^{prop.}$ decreases with increasing the loading rate, this descending trend has been interestingly diminished

Table 1
R-Curve characteristics for glass/epoxy and glass/CNF/epoxy composites at various loading rates.

Rate	Glass/epoxy composites			glass/CNF/epoxy composites		
	$G_{Ic}^{Ini.}$(± SDV) J/m^2	$G_{Ic}^{Prop.}$(± SDV) J/m^2	l_{FPZ}^{SS}(± SDV) mm	$G_{Ic}^{Ini.}$(± SDV) J/m^2	$G_{Ic}^{Prop.}$(± SDV) J/m^2	l_{FPZ}^{SS}(± SDV) mm
QS (1 mm/min)	144.3 (± 8.6)	612.3 (± 38.6)	22.3 (± 3.1)	192.5 (± 2.4)	695.3 (± 28.5)	15.8 (± 1.6)
50 mm/sec	130.5 (± 7.1)	555.5 (± 24.3)	16.2 (± 4.8)	181.8 (± 11.7)	659.7 (± 40.7)	18.4 (± 3.6)
100 mm/sec	141.7 (± 1.4)	508.1 (± 37.7)	14.8 (± 2.1)	172.9 (± 6.2)	639.5 (± 24.0)	17.6 (± 4.5)
200 mm/sec	143.2 (± 8.7)	482.3 (± 42.5)	13.5 (± 2.7)	178.5 (± 2.5)	639.8 (± 30.0)	15.4 (± 4.4)

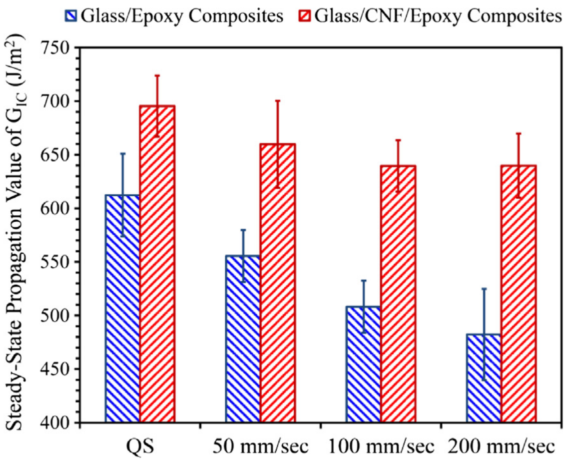

Fig. 7. Steady-state values of the strain energy release rate for both glass/epoxy and glass/CNF/epoxy composite specimens at different loading rates.

due to CNFs incorporation. While unmodified samples undergo a drop in $G_{Ic}^{Prop.}$ by more than 21% at 200 mm/sec loading rate, a slight reduction of less than 8% was observed in $G_{Ic}^{Prop.}$ of the glass/CNF/epoxy composite samples at the highest rate.

3.3. The crack tip rate analysis

In a number of previous research works concerning the rate dependency of G_{IC}, the results were expressed in correlation with the local opening rate at the crack tip [4,5,11] which differs from the applied far-field loading rate and does not remain constant during the crack propagation. The crack tip opening rate seems to be the most appropriate measure for rate dependency analysis of delamination growth [1]. Using the classical beam theory, Smiley [4] defined an expression for the crack opening displacement rate, $\dot{y}(x)$, at a distance x from the crack tip as:

$$\dot{y}(x) = \dot{\delta}(3ax^2 - x^3)/2a^3 \tag{1}$$

where $\dot{\delta}$ is the applied loading rate and a is the current delamination length prior to the crack propagation. At the crack tip, $x = 0$, the rate prior to crack propagation vanishes, $\dot{y}(0) = 0$. Therefore, the crack tip opening rate, $\dot{y}_{ct}$, is considered at some arbitrarily small distance, $x = \varepsilon$, from the crack tip. While $\varepsilon \ll a$, $\dot{y}_{ct}$ is simplified to a function of the test rate and delamination length as:

$$\dot{y}_{ct} = 3\dot{\delta}\varepsilon^2/2a^2 \tag{2}$$

which shows that the crack tip opening rate decreases during the crack evolution. Also, ε is normally chosen to be two times of a ply thickness.

This approach was tried in the present study to further elaborate on the rate sensitivity of the fracture toughness. The discrepancy of the strain energy release rate data points in the steady-state propagation phase of delamination growth, normalized with respect to the average quasi-static value ($G_{Ic}/G_{Ic}^{Prop.(QS)}$), versus $\dot{y}_{ct}$ are presented in Fig. 8(a), (b) for the glass/epoxy and glass/CNF/epoxy composite specimens, respectively. A clear descending trend of the fracture toughness with increasing the crack tip opening rate was found for the unmodified composite specimens. Similar behavior has been reported for the crack tip rate dependency of the fracture toughness in carbon/epoxy composites [11]. On the other hand, the variation of the normalized fracture toughness versus crack tip opening rate in Fig. 8(b) specifies a noteworthy reduction in the rate sensitivity due to adding CNFs to the composites.

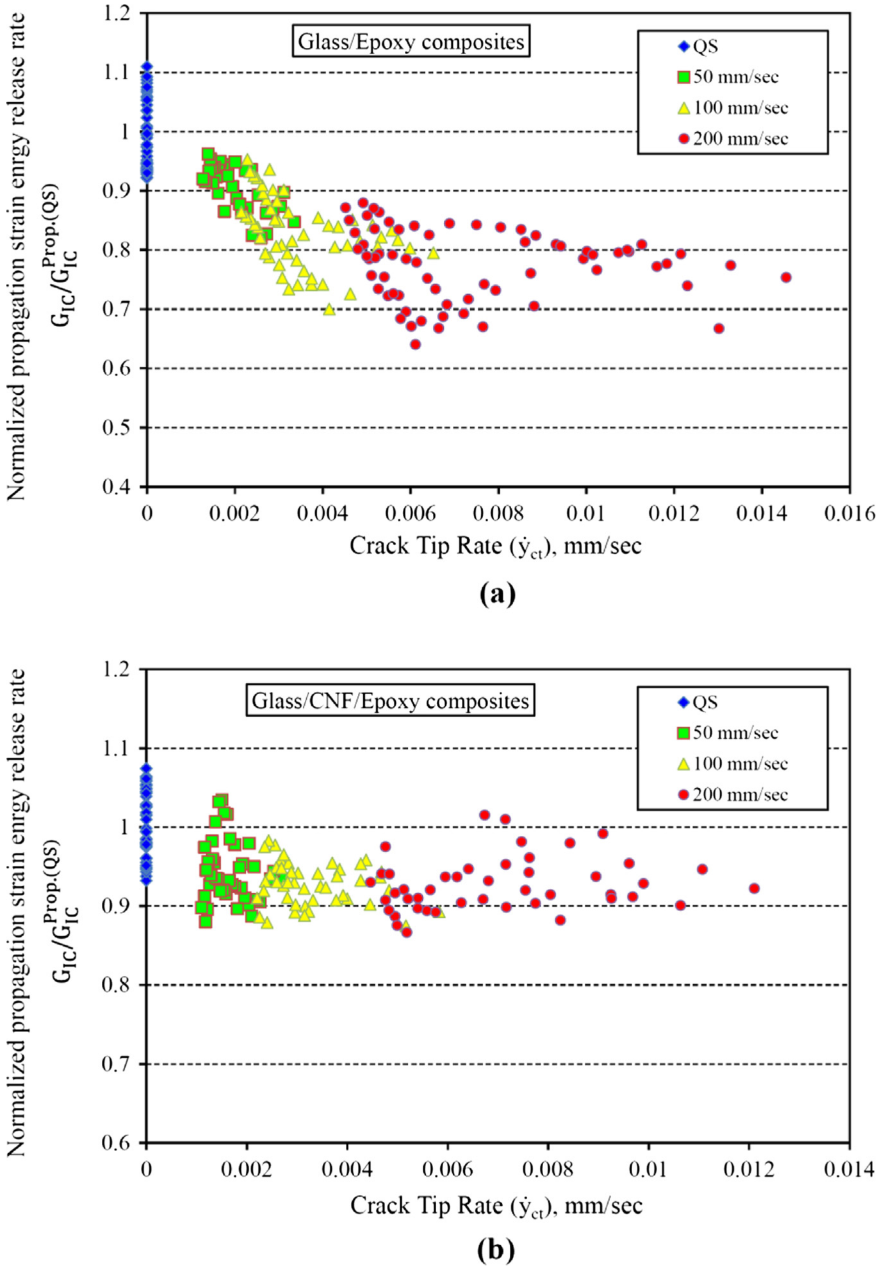

Fig. 8. Normalized propagation fracture toughness versus crack tip opening rate for (a) glass/epoxy and (b) glass/CNF/epoxy composite specimens.

3.4. Fractography inspection

In order to shed some light on the rate effects on the damage mechanisms that occur during the delamination growth and provide a physical explanation for the results, macroscopic fractography analysis of the upper and lower delaminated surfaces was performed for all the specimens tested at a minimum and maximum loading rates. For the glass/epoxy composites, different fracture surface appearances and detected damage mechanisms at two mentioned rates, can reasonably support the main idea of the reduced extent of fiber bridging and energy dissipation at high rates. The fracture surface inspection of the glass/epoxy composites at quasi-static tests is illustrated in Fig. 9. In quasi-static tests, features like widespread long bundles of peeled-off fibers and resulted rough fracture surfaces in the matrix along with numerous exposed, damaged and pulled-out fibers signify a dominant adhesion failure at the fiber/matrix interface and justify the observed extensive fiber bridging.

On the contrary, fracture surfaces of specimens tested at high rates show less amount of fiber exposure and adhesive failure at fiber/matrix bondings as shown in Fig. 10. Large areas of smooth fracture surfaces indicate a great tendency to the cleavage fracture

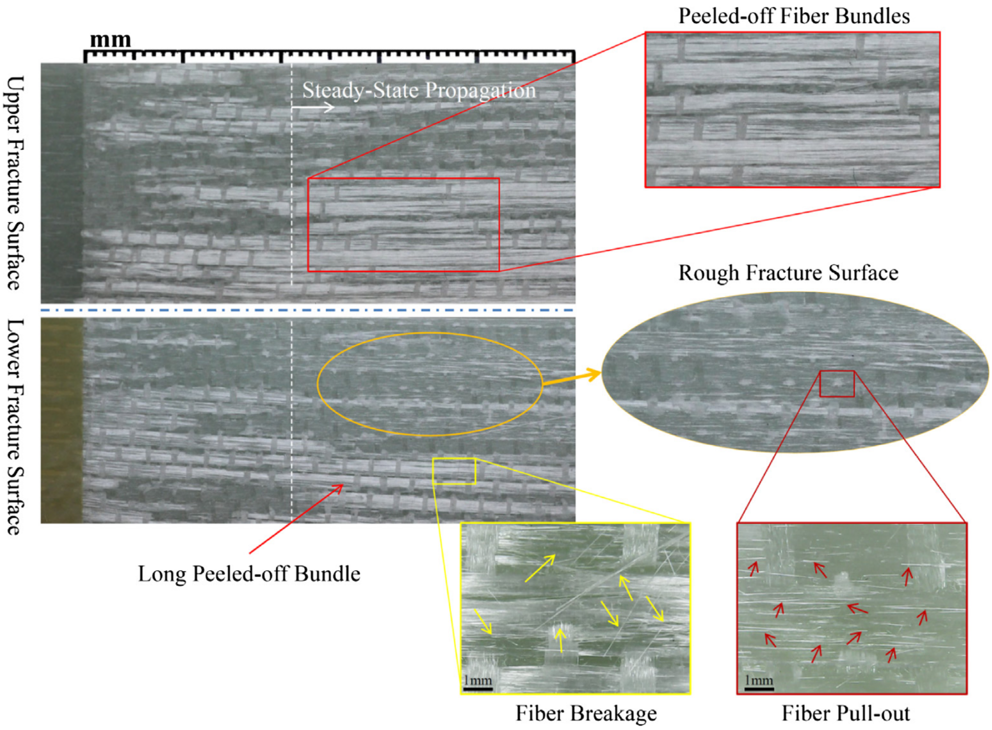

Fig. 9. The fracture surface inspection of the glass/epoxy composite specimen at a quasi-static loading rate.

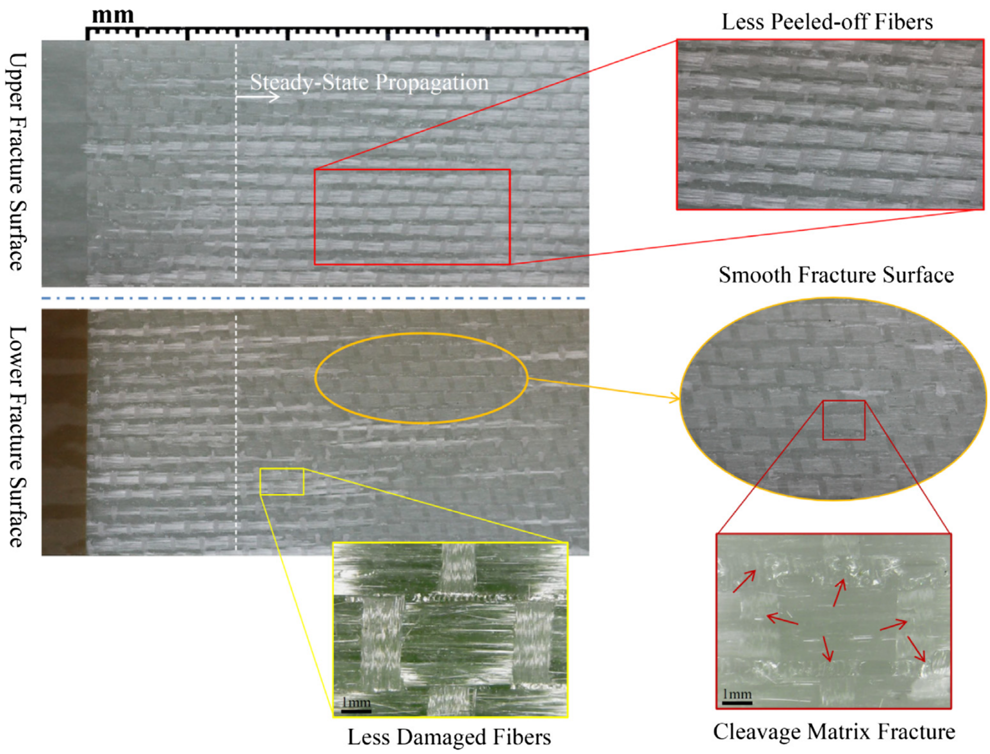

Fig. 10. Fracture surface inspection of the glass/epoxy composite specimen at 200 mm/sec loading rate.

of the epoxy matrix rather than the propagation of the crack at the fiber/matrix interface. Smooth matrix cleavage at elevated rates leads to lower values of the strain energy release rate in the steady-state region of the R-curve. A similar transition from ductile to brittle behavior was observed by Sun et al. [39] for the fracture of adhesively-bonded DCB joints tested at high loading rates. Larger

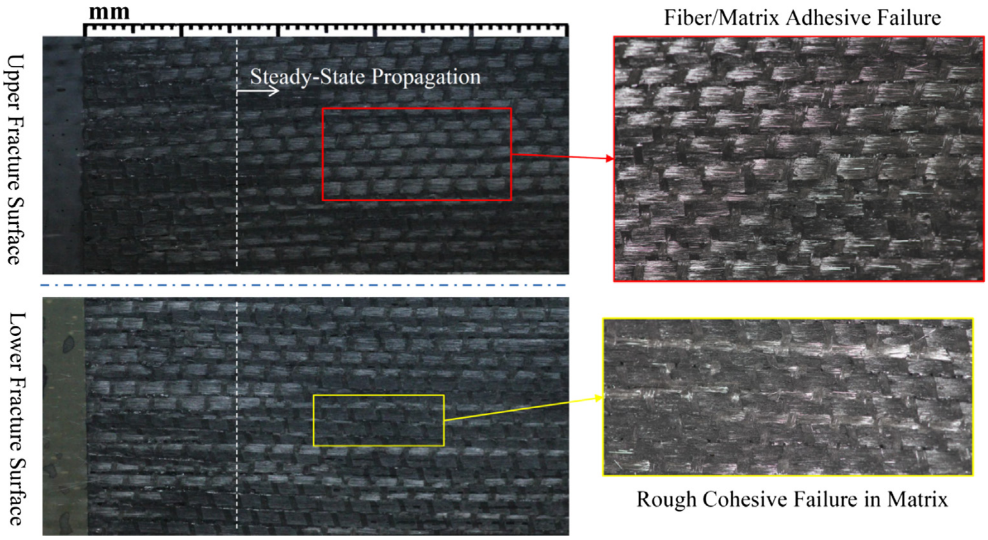

Fig. 11. The fracture surface of a glass/CNF/epoxy composite specimen tested at a 200 mm/sec loading rate.

areas of the matrix brittle fracture and less fiber/matrix debonding were previously introduced as a reason for the reduction of the fracture toughness at high loading rates [9]. Moreover, the smaller fiber bridging zone because of increased loading rate which was derived based on R-curve analysis can be physically verified by fewer amounts of either peeled-off or pulled-out fibers.

The observed tendency to cleavage matrix fracture and a smaller amount of fiber/matrix interface failure at elevated loading rates strengthen the idea followed in the present study that nano-reinforcement techniques can be advantageous to delamination resistance over a wide range of loading rates. In accordance with previous studies [24,40–42], the improved interlaminar fracture properties due to CNF incorporation can be contributed to two main factors: enhanced matrix toughness and improved fiber–matrix bonding. In presence of nano-reinforcements, the more favorable matrix-dominated fracture behavior can be related to further energy dissipation on account of more areas of rough fracture surfaces in the matrix and the effect of those long nanofillers either pulled from the matrix or bridged over the matrix cracks [24,28,43]. On the other hand, matrix modification can even promote enhanced interfacial bonding between fibers and matrix [24].

Based on the fracture surface inspections (Fig. 11), it seems that resin modification induced a balance between adhesive fiber/matrix debonding and cohesive matrix failure which does not appear to be rate sensitive. Increased toughness of the matrix, which can be recognized from amplified regions of textured fracture surfaces in the matrix, is a result of the pull-out and breakage of nanofibers in addition to their bridging over the matrix cracks as demonstrated in reference [21]. The roughness of the fracture surfaces in glass/CNF/epoxy composite samples remains comparatively unchanged at various loading rates. This finding exhibits that participations of the extrinsic toughening mechanisms governing the delamination growth in these specimens are not remarkably rate-sensitive within the range studied here. On the other hand, moderate fiber failure and fiber pull-out in both minimum and maximum loading rates comparing to the quasi-static fracture surfaces of glass/epoxy composites can be a sign of improved bondings between fibers and matrix. Better bondings increase the required load to peel-off and pull-out the fibers and consequently enhance the interlaminar fracture toughness. The less extended area of damage in a glass/polyester composite containing 0.2 wt% of CNFs, under low-velocity transverse impact was similarly clarified with better fiber/matrix bondings and the crack tip arrest by means of toughening the matrix [41,44].

4. Conclusion

An experimental investigation of the loading rate effects on mode-I delamination behavior of glass/epoxy and glass/CNF/epoxy laminated composites was conducted through performing experiments on DCB samples at four different crosshead speeds up to 200 mm/sec. For the manufacturing of glass/CNF/epoxy specimens, 0.25 wt% of CNFs were homogeneously mixed with the resin and then used for impregnation at the middle six layers of the composite plate using the hand lay-up process. The rate sensitivity analysis of the interlaminar fracture in the glass/epoxy composites along with examining resin nano-modification as a potential candidate to increase G_{IC} and diminish the loading rate dependency were the main objectives of the present research.

The glass/epoxy specimens showed a descending trend of the propagation fracture toughness and process zone length with increasing the loading rate. This rate dependency became clearer when the variation of the fracture toughness was plotted against the local crack tip opening rate. Based on macroscopic fractographic observations, the reduced interlaminar fracture resistance at elevated rates can be elucidated via less fiber/matrix interface failure, less contribution of fibers in energy dissipation during the crack growth, and enlarged areas of the brittle matrix fracture altering the fracture surface texture. For glass/CNF/epoxy specimens, G_{IC} was enhanced in comparison with glass/epoxy samples, as well as limited loading rate sensitivity was interestingly observed in the results. The findings of this research demonstrate the potential of resin modification using nanofillers to enhance the interlaminar fracture toughness and reduce the loading rate dependency.

Uncited Reference

[35]

Declaration of Competing Interest

The authors declare that they have no known competing financial interests or personal relationships that could have appeared to influence the work reported in this paper.

References

[1] May M. Measuring the rate-dependent mode I fracture toughness of composites – a review. Compos Part A Appl Sci Manuf 2016;81:1–12. https://doi.org/10.1016/j.compositesa.2015.10.033.
[2] American Society for Testing and Materials (ASTM). Standard Test Method for Mode I Interlaminar Fracture Toughness of Unidirectional. Annu B ASTM 2004;03:1–12. 10.1520/D5528-01R07E03.2.
[3] Aliyu AA, Daniel IM. Effects of strain rate on delamination fracture toughness of graphite/epoxy. Delaminat Debond Mater ASTM STP 1985;876:336–48.
[4] Smiley RBP AJ. Rate effects on mode I interlaminar fracture toughness in composite materials. J. Compos. Mater. 1987;21:670–87. https://doi.org/10.1177/002199838702100706.
[5] Mall S, Law GE, Katouzian M. Loading rate effect on interlaminar fracture toughness of a thermoplastic composite. J. Compos. Mater. 1987;21:569–79. https://doi.org/10.1177/002199838702100607.
[6] Daniel IM, Shareef I, Aliyu AA. Rate effects on delamination fracture toughness of a toughened graphite/epoxy. ASTM Spec. Tech. Publ. 1987:260–74.
[7] You H, Yum Y-J. Loading rate effect on mode i interlaminar fracture of carbon/epoxy composite. J. Reinf. Plast. Compos. 1997;16:537–49. https://doi.org/10.1177/073168449701600604.
[8] Blackman BRK, Dear JP, Kinloch AJ, Macgillivray H, Wang Y, Williams JG, et al. The failure of fibre composites and adhesively bonded fibre composites under high rates of test. J. Mater. Sci. 1995;30:5885–900. https://doi.org/10.1007/BF01151502.
[9] Zabala H, Aretxabaleta L, Castillo G, Aurrekoetxea J. Loading rate dependency on mode I interlaminar fracture toughness of unidirectional and woven carbon fibre epoxy composites. Compos. Struct. 2015;121:75–82. https://doi.org/10.1016/j.compstruct.2014.11.001.
[10] Colin de Verdiere M, Skordos AA, May M, Walton AC. Influence of loading rate on the delamination response of untufted and tufted carbon epoxy non crimp fabric composites: mode I. Engng. Fract. Mech. 2012;96:11–25. https://doi.org/10.1016/j.engfracmech.2012.05.015.
[11] Thorsson SI, Waas AM, Schaefer J, Justusson B, Liguore S. Effects of elevated loading rates on mode I fracture of composite laminates using a modified wedge-insert fracture method. Compos. Sci. Technol. 2018;156:39–47. https://doi.org/10.1016/j.compscitech.2017.12.018.
[12] Yaniv G, Daniel IM. Height-tapered double cantilever beam specimen for study of rate effects on fracture toughness of composites. ASTM Spec. Tech. Publ. 1988:241–58. https://doi.org/10.1520/STP26139S.
[13] Gillespie JW, Carlsson LA, Smiley AJ. Rate-dependent mode I interlaminar crack growth mechanisms in graphite/epoxy and graphite/PEEK. Compos. Sci. Technol. 1987;28:1–15. https://doi.org/10.1016/0266-3538(87)90058-3.
[14] Beguelin P, Barbezat M, Kausch HH. Mechanical characterization of polymers and composites with a servohydraulic high-speed tensile tester. J Phys III 1991(1):1867–80. https://doi.org/10.1051/jp3:1991238.
[15] Benmedakhene S, Kenane M, Benzeggagh ML. Initiation and growth of delamination in glass/epoxy composites subjected to static and dynamic loading by acoustic emission monitoring. Compos Sci Technol 1999;59:201–8. https://doi.org/10.1016/S0266-3538(98)00063-3.
[16] Shokrieh MM, Heidari-Rarani M, Ayatollahi MR. Delamination R-curve as a material property of unidirectional glass/epoxy composites. Mater Des 2012;34:211–8. https://doi.org/10.1016/j.matdes.2011.08.006.
[17] Shokrieh MM, Salamat-talab M, Heidari-Rarani M. Effect of interface fiber angle on the R-curve behavior of E-glass/epoxy DCB specimens. Theor Appl Fract Mech 2016;86:153–60. https://doi.org/10.1016/j.tafmec.2016.06.006.
[18] Cantwell WJ, Kausch HH. An evaluation of the interlaminar fracture toughness of a thermoplastic composite with offset centre flies. Mech Compos Mater 1993;28:328–33. https://doi.org/10.1007/BF00616160.
[19] Cantwell WJ, Blyton M. Influence of loading rate on the interlaminar fracture properties of high performance composites – a review. Appl Mech Rev 1999;52:199. https://doi.org/10.1115/1.3098934.
[20] Ladani RB, Bhasin M, Wu S, Ravindran AR, Ghorbani K, Zhang J, et al. Fracture and fatigue behaviour of epoxy nanocomposites containing 1-D and 2-D nanoscale carbon fillers. Engng Fract Mech 2018;203:102–14. https://doi.org/10.1016/j.engfracmech.2018.04.033.
[21] Silva H, Ferreira JAM, Capela C, Richardson MOW. Mixed mode interlayer fracture of glass fiber/nano-enhanced epoxy composites. Compos Part A Appl Sci Manuf 2014;64:211–22. https://doi.org/10.1016/j.compositesa.2014.05.011.
[22] Wang P, Liu W, Zhang X, Lu X, Yang J. Enhanced fracture toughness of carbon fabric/epoxy laminates with pristine and functionalized stacked-cup carbon nanofibers. Engng Fract Mech 2015;148:73–81. https://doi.org/10.1016/j.engfracmech.2015.09.010.
[23] Hsiao K-T, Scruggs AM, Brewer JS, Hickman GJS, McDonald EE, Henderson K. Effect of carbon nanofiber z-threads on mode-I delamination toughness of carbon fiber reinforced plastic laminates. Compos Part A Appl Sci Manuf 2016;91:324–35. https://doi.org/10.1016/j.compositesa.2016.10.022.
[24] Zhu Y, Bakis CE, Adair JH. Effects of carbon nanofiller functionalization and distribution on interlaminar fracture toughness of multi-scale reinforced polymer composites. Carbon N Y 2012;50:1316–31. https://doi.org/10.1016/j.carbon.2011.11.001.
[25] Lubineau G, Rahaman A. A review of strategies for improving the degradation properties of laminated continuous-fiber/epoxy composites with carbon-based nanoreinforcements. Carbon N Y 2012;50:2377–95. https://doi.org/10.1016/j.carbon.2012.01.059.
[26] Wu S, Ladani RB, Ravindran AR, Zhang J, Mouritz AP, Kinloch AJ, et al. Aligning carbon nanofibres in glass-fibre/epoxy composites to improve interlaminar toughness and crack-detection capability. Compos Sci Technol 2017;152:46–56. https://doi.org/10.1016/j.compscitech.2017.09.007.
[27] Tsantzalis S, Karapappas P, Vavouliotis A, Tsotra P, Kostopoulos V, Tanimoto T, et al. On the improvement of toughness of CFRPs with resin doped with CNF and PZT particles. Compos Part A Appl Sci Manuf 2007;38:1159–62. https://doi.org/10.1016/j.compositesa.2006.04.016.
[28] Palmeri MJ, Putz KW, Ramanathan T, Brinson LC. Multi-scale reinforcement of CFRPs using carbon nanofibers. Compos Sci Technol 2011;71:79–86. https://doi.org/10.1016/j.compscitech.2010.10.006.
[29] Zhou Y, Pervin F, Rangari VK, Jeelani S. Fabrication and evaluation of carbon nano fiber filled carbon/epoxy composite. Mater Sci Engng A 2006;426:221–8. https://doi.org/10.1016/j.msea.2006.04.031.
[30] Shi D-L, Feng X-Q, Huang YY, Hwang K-C, Gao H. The effect of nanotube waviness and agglomeration on the elastic property of carbon nanotube-reinforced composites. J Engng Mater Technol 2004;126:250–7. https://doi.org/10.1115/1.1751182.
[31] Shokrieh MM, Esmkhani M, Vahedi F, Shahverdi HR. Improvement of mechanical and electrical properties of epoxy resin with carbon nanofibers. Iran Polym J 2013;22:721–7. https://doi.org/10.1007/s13726-013-0170-2.
[32] Shokrieh MM, Esmkhani M, Haghighatkhah AR. Flexural fatigue behaviour of carbon nanofiber/epoxy nanocomposites. Fatigue Fract Engng Mater Struct 2014;37:553–60. https://doi.org/10.1111/ffe.12137.
[33] Chitsazzadeh M, Shahverdi H, Shokrieh MM. Fabrication of multi-walled carbon nanotube/vinyl ester nanocomposites: dispersion and stabilization. Defect Diffus Forum 2011;312–315:460–5. https://doi.org/10.4028/www.scientific.net/DDF.312-315.460.
[34] Amaral L, Alderliesten R, Benedictus R. Towards a physics-based relationship for crack growth under different loading modes. Engng Fract Mech

2018;195:222–41. https://doi.org/10.1016/j.engfracmech.2018.04.017.
[35] Daneshjoo Z, Shokrieh MM, Fakoor M, Alderliesten R, Zarouchas D. Physics of delamination onset in unidirectional composite laminates under mixed-mode I/II loading. Engng Fract Mech 2019;211:82–98. https://doi.org/10.1016/j.engfracmech.2019.02.013.
[36] Montenegro DM, Pappas G, Botsis J, Zogg M, Wegener K. A comparative study of mode I delamination behavior of unidirectional glass fiber-reinforced polymers with epoxy and polyurethane matrices using two methods. Engng Fract Mech 2019;206:485–500. https://doi.org/10.1016/j.engfracmech.2018.12.008.
[37] Shokrieh MM, Salamat-talab M, Heidari-Rarani M. Dependency of bridging traction of DCB composite specimen on interface fiber angle. Theor Appl Fract Mech 2017;90:22–32. https://doi.org/10.1016/j.tafmec.2017.02.009.
[38] Ekhtiyari A. Loading rate effects on the Mode I delamination growth of laminated Glass/epoxy and Glass/CNF-modified epoxy DCB specimens. 4TUCentre Res Data Dataset 2019. 10.4121/uuid:1e7fe12a-c5a1-4840-a24c-2ba977783e1b.
[39] Sun C, Thouless MD, Waas AM, Schroeder JA, Zavattieri PD. Ductile–brittle transitions in the fracture of plastically-deforming, adhesively-bonded structures. Part I: experimental studies. Int J Solids Struct 2008;45:3059–73. https://doi.org/10.1016/j.ijsolstr.2008.01.011.
[40] Bortz DR, Merino C, Martin-Gullon I. Mechanical characterization of hierarchical carbon fiber/nanofiber composite laminates. Compos Part A Appl Sci Manuf 2011;42:1584–91. https://doi.org/10.1016/j.compositesa.2011.07.002.
[41] Hossain MK, Hossain ME, Dewan MW, Hosur M, Jeelani S. Effects of carbon nanofibers (CNFs) on thermal and interlaminar shear responses of E-glass/polyester composites. Compos Part B Eng 2013;44:313–20. https://doi.org/10.1016/j.compositesb.2012.05.006.
[42] Ladani RB, Ravindran AR, Wu S, Pingkarawat K, Kinloch AJ, Mouritz AP, et al. Multi-scale toughening of fibre composites using carbon nanofibres and z-pins. Compos Sci Technol 2016;131:98–109. https://doi.org/10.1016/j.compscitech.2016.06.005.
[43] Wicks SS, Wang W, Williams MR, Wardle BL. Multi-scale interlaminar fracture mechanisms in woven composite laminates reinforced with aligned carbon nanotubes. Compos Sci Technol 2014;100:128–35. https://doi.org/10.1016/j.compscitech.2014.06.003.
[44] Hossain ME, Hossain MK, Hosur M, Jeelani S. Low-velocity impact behavior of CNF-filled glass-reinforced polyester composites. J Compos Mater 2014;48:879–96. https://doi.org/10.1177/0021998313480194.